PROF. SEONGMIN LEE (Orcid ID : 0000-0001-6635-8775)

Article type : Research Article

Synthesis, Structure, and Biological Evaluation of a Platinum-Carbazole Conjugate

Young Cheun,[1*] *Myong-Chul Koag,*[1*] *Youssef W. Naguib,*[2,3] *Hala Ouzon-Shubeita,*[1] *Zhengrong Cui,*[2] *Danaya Pakotiprapha,*[4] *and Seongmin Lee*[1]

[1]Division of Chemical Biology and Medicinal Chemistry, College of Pharmacy, The University of Texas at Austin, Austin, TX 78712, United States

[2]Division of Pharmaceutics, College of Pharmacy, The University of Texas at Austin, Austin, TX 78712, United States

[3]Department of Pharmaceutics, Faculty of Pharmacy, Minia University, Minia, Egypt

[4]Department of Biochemistry and Center of Excellence in Protein and Enzyme Technology, Faculty of Science, Mahidol University, Bangkok 10400, Thailand

*These authors equally contributed to the work.

Corresponding Author

Seongmin Lee, [1]Division of Chemical Biology and Medicinal Chemistry, College of Pharmacy, The University of Texas at Austin, Austin, TX 78712, United States

Phone: +1 (512) 471-1785

Email: seongminlee@austin.utexas.edu

This article has been accepted for publication and undergone full peer review but has not been through the copyediting, typesetting, pagination and proofreading process, which may lead to differences between this version and the Version of Record. Please cite this article as doi: 10.1111/cbdd.13062

KEYWORDS: DNA damage, Cisplatin, X-ray crystallography, Nucleotide excision repair, Cancer therapy

ABSTRACT

Cisplatin resistance is caused, in part, by the efficient removal of the helix-distorting cisplatin 1,2-intrastrand crosslinks by nucleotide excision repair (NER) machinery. To make a platinum-DNA adduct that causes less helical distortion than the cisplatin 1,2-intrastrand adduct, we designed and synthesized a monofunctional platinum-carbazole conjugate (carbazoleplatin). The 2.5Å crystal structure of carbazoleplatin-DNA adduct revealed both the monoplatination of the N7 of a guanine (G) base and the intercalation into two G:C base pairs while causing a minor distortion of the DNA helix. A 50-mer dsDNA containing a single carbazoleplatin lesion was poorly processed by UvrABC endonuclease, the prokaryotic NER machinery that detects helical distortion and performs dual incision around the lesion. Our cell viability assay indicated that the cytotoxic pathways of carbazoleplatin might be different from those of cisplatin; carbazoleplatin was 5 to 8 times more cytotoxic than cisplatin against PANC-1 and MDA-MB-231 cancer cell lines.

INTRODUCTION

cis-Diamminedichloridoplatinum(II), previously *cis*-Diamminedichloroplatinum(II), or commonly cisplatin is a classical bifunctional platinum-based anticancer drug, which has been administered to more than half of chemotherapy patients (Figure 1).[1] While cisplatin targets multiple cellular targets, it has been widely accepted that DNA is the main target that gives the cytotoxicity.[2,3] Upon binding to the target DNA, cisplatin forms a complex with the N7 atoms of two guanines in close proximity, generating 1,2-intrastrand, 1,3-intrastrand, and interstrand crosslink adducts. The most predominant form (approximately 65%), 1,2-intrastrand crosslink, distorts the DNA helix by unwinding the helix and exposing the minor groove opposite to the lesion (verified by both NMR[4] and X-ray[5,6]), thus inhibiting transcription and replication and ultimately inducing apoptosis.[7,8]

Drug resistance is one of the major limitations of cisplatin-based chemotherapy. It has been reported that relapses occurred on most of the ovarian cancer patients who had been treated with cisplatin in about 15 months, leading to poor prognosis (15-20% survival in 5 years).[9,10] One mechanism of cisplatin resistance is the removal of cisplatin-DNA intrastrand crosslink adducts by nucleotide excision repair (NER) pathway.[8] Cisplatin-sensitive cancer cells were reported to exhibit low levels of NER proteins (e.g., XPA, ERCC-XRF), whereas increased NER activity was observed in cisplatin-resistant cancer cells.[7,11-13]

To circumvent cisplatin resistance, researchers explored the potential of new structural motifs that deviate from the traditional structure-activity relationship (SAR) guidelines.[14,15] Among those motifs, polynuclear platinum agent, monofunctional platinum agent, and platinum-intercalator conjugate have shown some promising preclinical results (Figure 1).[16] Originally intended to study biophysical properties of DNA[17] and to explore the potential synergism between cisplatin and doxorubicin,[18] platinum-intercalator conjugate is now a viable concept to overcome cisplatin resistance.[19-21] A platinum-intercalator conjugate is characterized by a platinum core and a DNA intercalator connected with a covalent linker, and in general, it is capable of inhibiting the replication while stabilizing the duplex structure of the target DNA.[16,22] Depending on the platinum core, the DNA intercalator, and the linker, the conjugate can exert different physical and biological outcomes. The laboratory of Ulrich Bierbach developed a platinum-acridine conjugate connected by a central 2-aminoethyl thiourea/guanidine linker (called Pt-ACRAMTU) that promotes the intercalation-driven platination by utilizing a strongly intercalating acridine moiety and a relatively rigid aminoethyl guanidine.[19] Pt-ACRAMTU is thought to stall DNA processing enzymes by unwinding and lengthening the DNA helix at the intercalation site while inducing small conformational changes of DNA,[23,24] and it was shown to be effective against several cancer cell lines.[19] The laboratory of Curt Davey developed a platinum-naphthylimide conjugate (called PtNAP), and its *cis*- and *trans*- isomers target different DNA sites in the nucleosome.[25] Both of the isomers were shown to be effective against a cisplatin-resistant cancer cell line.[25]

In conjunction with our efforts to develop a platinum-based anticancer agent that can be slowly removed by NER, herein we report the synthesis, the structure, and the bioactivity of a novel platinum-carbazole conjugate connected with an ethylene diamine linker (hereafter called carbazoleplatin); in contrast to Pt-ACRAMTU or PtNAP, our molecule uses an aromatic heterocycle that had not been previously used as a DNA intercalator and a more flexible, compact covalent linker. We evaluated carbazoleplatin's mode of interaction by obtaining a crystal structure of carbazoleplatin-DNA adduct using the pol β host-guest system that we had recently developled in our laboratory.[26] We also tested how a UvrABC complex (the prokaryotic NER) removes a carbazoleplatin adduct from its DNA substrate and how cancer cells respond to carbazoleplatin.

1. EXPERIMENTAL SECTION

1.1. Chemistry

1.1.1. Preparation of 2-(*9H*-carbazol-9-yl)ethan-1-ol. Commercially available starting material carbazole (3.34 g, 20.0 mmol) was dissolved in acetone (40 mL, 0.5M). Finely crushed potassium hydroxide (KOH, 7.0 g, 6.3 mmol) was added to the solution. The mixture was stirred at room temperature for 30 minutes, and then 2-bromoethanol (1.4 mL, 1.25 equiv) was added to the mixture dropwise. The reaction mixture was refluxed at 60ºC under argon gas for 18 hours in the dark. Once the product formation was determined via thin layer chromatography, the solvent was removed *in vacuo*. The mixture was subject to work-up (ethyl acetate/water), and the resulting organic layer was washed with brine and dried over sodium sulfate. The crude mixture was purified via silica gel column chromatography (4:1 hexane/ethyl acetate) to afford the desired product as brown solids (1.34 g, 6.3 mmol, 32%). Cleaner reaction and improved yield could be obtained with the use of sodium hydride instead of KOH. in acetone. ^{1}H NMR ($CDCl_3$) spectrum is available. ^{1}H NMR (CDCl3, 400 MHz): δ 8.11 (2H, d, J = 7.9 Hz), 7.47 (4H, m), 7.25 (2H, m), 4.50 (2H, t, J = 5.5 Hz), 4.09 (2H, m).

1.1.2. Preparation of 9-(2-azidoethyl)-carbazole. The starting material 2-(*9H*-carbazol-9-yl)ethan-1-ol (1.8 g, 8.5 mmol) was dissolved in tetrahydrofuran (THF, 85 mL, 0.1 M). Triphenyl phosphine (4.46 g, 2.0 equiv) and imidazole (2.9 g, 5.0 equiv) were added to the solution. While stirring the mixture at room temperature, iodine chips (4.5 g, 2.1 equiv) were added to the mixture in one portion. The mixture was stirred for 30 minutes. Once the product formation was determined via thin layer chromatography, aqueous sodium thiosulfate was added to the mixture until the color disappeared. The reaction mixture was subject to work-up (ethyl acetate/water), and the resulting organic layer was washed with brine and dried over sodium sulfate. The crude mixture was purified via silica gel column chromatography (8:1 hexane/ethyl acetate) to afford the desired iodide. The iodide was dissolved in *N,N*-dimethylformamide (DMF, 50 mL), and sodium azide (5.5 g 10.0 equiv) was added to the DMF solution. The mixture was refluxed at 70ºC under argon for 1 day. Once the product formation was determined via thin layer chromatography, the solvent was removed *in vacuo*. The reaction mixture was subject to work-up (ethyl acetate/water), and the resulting organic layer was washed with brine and dried over sodium sulfate. The crude mixture was purified via silica gel column chromatography to afford the desired azide as yellow solids (2.03 g, 8.6 mmol, 100%). ^{1}H NMR ($CDCl_3$) spectrum is available. ^{1}H NMR ($CDCl_3$, 400 MHz): δ 8.11 (2H, t, J = 7.9 Hz), 7.47 (4H, m), 7.27 (2H, m), 4.50 (2H, t, J = 6.2 Hz), 3.74 (2H, t, J = 6.16 Hz).

1.1.3. Preparation of 2-(*9H*-carbazol-9-yl)ethan-1-amine. The starting material 9-(2-azidoethyl)-carbazole (840 mg, 3.6 mmol) was dissolved in tetrahydrofuran (THF, 35 mL, 0.1 M). Triphenyl phosphine (2.8 g, 3.0 equiv), and then water (0.64 mL, 10.0 equiv) were added to the solution, and the mixture was stirred at room temperature for 16 hours. Once the product formation was determined via thin layer chromatography, the reaction mixture was subject to work-up (ethyl acetate/water). The resulting organic layer was washed with brine and dried over sodium sulfate. The crude mixture was purified via silica gel column chromatography (6:1 hexane/ethyl acetate) to afford the desired product as yellow oil (433 mg, 2.1 mmol, 58%). ^{1}H NMR ($CDCl_3$ and DMSO-d_6) spectra are available. ^{1}H NMR ($CDCl_3$, 400 MHz): δ 8.11 (2H, d, J =7.9 Hz), 7.47 (4H, d, J = 3.8 Hz), 7.25 (2H, m), 4.42 (2H, t, J = 6.2 Hz), 3.23 (2H, t, J = 6.2 Hz), 1.52 (2H, br). ^{1}H NMR (DMSO-d_6, 400

MHz): δ 8.12 (2H, d, J = 7.9 Hz), 7.61 (2H, d, J = 8.2 Hz), 7.42 (2H, t, J = 7.2 Hz), 7.16 (2H, t, J = 7.2 Hz), 4.34 (2H, t, J = 6.8 Hz), 2.91 (2H, d, J = 6.8 Hz).

1.1.4. Preparation of carbazoleplatin. *Cis*-dichlorodiamminoplatinum(II) (619 mg, 1.0 equiv) was dissolved in *N,N*-dimethylformamide (DMF, 33 mL). Silver nitrate (350 mg, 1.0 equiv) was added to the solution in the dark, and the mixture was stirred at 55ºC under argon gas for 1 day. The reaction mixture was filtered though 20 μm nylon filter to remove insolubles. The filter cake was washed with DMF. The clear and colorless filtrate was transferred to a new flask. To the flask, the starting material 2-(*9H*-carbazol-9-yl)ethan-1-amine (433 mg, 2.06 mmol) was added to the mixture. The new reaction mixture was stirred at 55ºC under argon gas in the dark. After 1 additional day, the reaction mixture was taken out from the heat source and the solvent was removed *in vacuo*. The crude mixture was dissolved in minimum volume of methanol. 10× (by volume) cold diethyl ether was poured to the methanol. The resulting white solids were collected and further purified with additional methanol/ether wash. ^{1}H NMR (DMSO-d_6), ^{13}C NMR (DMSO-d_6), ^{195}Pt NMR (DMSO-d_6), and hrMS (ESI) spectra are available. ^{1}H NMR (DMSO-d_6, 400 MHz): δ 8.15 (2H, d, J = 7.5 Hz), 7.65 (2H, d, J = 7.9 Hz), 7.48 (2H, t, J = 7.2 Hz), 7.20 (2H, t, J = 7.5 Hz), 5.10 (2H, br), 4.63 (2H, t), 4.31 (3H, br), 3.99 (3H, br), 2.92 (2H, m). ^{13}C NMR (DMSO-d_6, 150 MHz): δ 139.8, 125.9, 122.2, 120.4, 119.1, 109.0, 43.3, 42.2. ^{195}Pt NMR (DMSO-d_6, 129 MHz): δ –2390. hrMS (ESI): chemical formula: $C_{14}H_{20}ClN_4Pt^+$, calculated m/z 474.1024, observed m/z 474.1020.

1.2. Structure Characterization of Carbazoleplatin

1.2.1. Structure Determination of Carbazoleplatin. The crystals grew as colorless plates by methanol:diethyl ether vapor diffusion. The crystal was cut from a larger fragment and had approximate dimensions; 0.18 × 0.11 × 0.04 mm. The data were collected on an Agilent Technologies SuperNova Dual Source diffractometer using a μ-focus Cu Kα radiation source (λ = 1.5418Å) with collimating mirror monochromators. A total of 989 frames of data were collected using w-scans with a scan range of 1° and a counting time of 2 seconds per frame with a detector offset of ± 41.0° and 5 seconds per frame with a detector offset of ± 108.3°. The data were collected

at 100 Kusing an Oxford Cryostream low temperature device. Data collection, unit cell refinement and data reduction were performed using Agilent Technologies CrysAlisPro. The structure was solved by direct methods using SuperFlip and refined by full-matrix least-squares on F^2 with anisotropic displacement parameters for the non-H atoms using SHELXL-2013. Structure analysis was aided by use of the programs PLATON98 and WinGX. The hydrogen atoms were calculated in ideal positions with isotropic displacement parameters set to 1.2 × Ueq of the attached atom.

1.2.2. Structure Determination of Carbazoleplatinated DNA using pol *β* Host-Guest Complex. Human DNA polymerase β (pol *β*) was expressed and purified from *Escherichia coli* as described previously,[27,28] 16-mer template (5'-CCG ACG GAG GAG CAG G-3'), 10-mer upstream (5'-CCT GCT CCT C-3'), and 5-mer downstream oligonucleotides (5'-phosphate/GTC GG-3') were purchased from Integrated DNA Technologies (Coralville, IA). Platinated upstream oligo was prepared as described previously with minor modifications.[29] Carbazoleplatin was aquated by adding 1.2 equivalent of $AgNO_3$ to 3.0 mM of carbazoleplatin in water. The mixture was vortexed in the dark at room temperature for 15 hours and centrifuged for 20 minutes at 13,000×g to collect the supernatant. 1.5 μmol of the unmodified upstream primer in 10 mM sodium phosphate buffer (pH 6.3) was mixed with the aquated carbazoleplatin at 1:1.1 molar ratio. Then, the mixture was incubated at 37ºC for 15 hours. The platinated primer was purified using a GE Healthcare Mono Q 5/50 GL ion exchange column in 10 mM Tris buffer (pH 8.0) with NaCl gradient from 0.1 to 1.0 M.[30] Then the purified primer was desalted using a Waters Corporation Sep-Pak C18 column (Milford, MA), dried, and reconstituted in water. The purified upstream primer, the phosphorylated downstream, and the template were annealed in 20 mM $MgCl_2$, 0.1 M Tris buffer (pH 7.5) to afford single-nucleotide gapped DNA as described.[27] The pol *β*-DNA host-guest complex crystals were grown in 50 mM imidazole, 14-23% PEG3400, and 350 mM sodium acetate at pH 7.5 as previously reported.[30] Crystals were cryo-protected in mother liquor supplemented with 12% ethylene glycol, and they were flash-frozen in liquid nitrogen. Diffraction data were collected at 100 K using either a Rigaku MicroMax-007 HF microfocus X-ray generator with R-Axis IV^{++}imaging plate area detector or the beamline 5.0.3 Advanced Light Source at Berkeley Center for Structural Biology. The diffraction data

were processed using HKL 2000.[31] The structures of the pol β-DNA host-guest complexes were solved by molecular replacement with pol β with a single-nucleotide gapped DNA (PDB ID 1BPX) as the search model. The model was built using COOT[32] and refined using PHENIX software.[33] Ramachandran plots were generated using MolProbity program.

1.2.3. DNA Torsion Analysis. We extracted the atom coordinates of the upstream complementary DNA and the corresponding template strand from the PDB file and analyzed distortion parameters using W3DNA (http://w3dna.rutgers.edu), a web based platform of the distortion analysis software 3DNA v2.0.[34]

1.3. Biological Properties of Carbazoleplatin

1.3.1. UvrABC Incision Assay. The laboratory of Danaya Pakotiprapha (Mahidol University, Thailand) has kindly given us the constructs of UvrA, UvrB, and UvrC. Purified UvrA, UvrB, and UvrC from *Bacillus stearothermophilus* were prepared as described previously.[35] Fluorescein-labeled template strand 5'-FAM/ CTC TCT CTT CTC TTT TCC CTC TCT TGX TCC TTC TCT CCC CTC TCC TCT CC-3' and its complementary strand 5′-GGA GAG GAG AGG GGA GAG AAG GAY CAA GAG AGG GAA AAG AGA AGA GAG AG-3′ (X and Y = C and G for the carbazoleplatin lesion, G and C for the cisplatin lesion) were purchased from Integrated DNA Technologies (Coralville, IA). Aquated carbazoleplatin and cisplatin were mixed with the corresponding template strand (platinum: DNA molar ratio = 2:1) in 10 mM sodium phosphate buffer (pH 6.8) and incubated at 37ºC in the dark for 18 hours. Each lesion-containing ssDNA was purified using a GE Healthcare Mono Q 5/50 GL ion exchange column in 10 mM Tris buffer (pH 8.0) with 3-step NaCl gradient (0.0 to 0.15 M for 0.5 column volume, 0.15 to 0.5 M for 25 column volume, 0.5 to 1.0 M for 0.5 column volume). The desired fractions were analyzed via 20% polyacrylamide urea gel electrophoresis. After the desalting, each lesion-containing ssDNA was annealed with the corresponding complementary strand by mixing them in 1:1 molar ratio and heating the mixture at 90ºC for 10 minutes followed by slow cooling. 40 nM of the annealed DNAs were pre-incubated with 500 nM UvrA and 500 nM UvrB in 50 mM Tris-HCl pH 7.5, 10 mM $MgCl_2$, 100 mM KCl, 0.1 μg/μl BSA, 1 mM ATP and 2%

glycerol at 37 °C for 2 minutes. Then, 500 nM of UvrC was added to each mixture. After 1 hour, each reaction was quenched with formamide loading buffer (95% formamide, 20 mM EDTA, pH 8.3, 0.1 mg/mL bromophenol blue, and 0.1 mg/mL xylene cyanol). The reaction products were denatured by heating the mixture at 90 °C for 5 min and separated by molecular weight via 20% polyacrylamide urea gel electrophoresis. The 6-carboxyfluorescein (6-FAM) dye was visualized using GE Life Sciences Typhoon FLA 9500 (excitation laser: 473 nm, emission filter: LPB). The intensity was quantified using ImageJ.[36]

1.3.2. MTT Cytotoxicity Assay. Carbazoleplatin and cisplatin were dissolved in RPMI1640 media (Invitrogen, Carlsbad, CA) to prepare stock solutions, then serial dilutions in media were made as 100, 10, 1, 0.1, 0.01, and 0.001 μM. Cells (PANC1 and MDA-MB-231, American Type Culture Collection, Manassas, VA) were seeded as 1500 cells/well for overnight (in 75 μL). On the second day, carbazoleplatin or cisplatin was added to the wells to final concentrations as aforementioned (75 μL per well, n = 4). After 48 hours of incubation at 37ºC with 5% CO_2, 20 μL of MTT reagent (5 mg/mL in PBS) were added, and the cells were incubated for two additional hours. All the aqueous media were removed, and 100 μL of dimethyl sulfoxide were added to dissolve the formed formazan crystals. After crystals were dissolved, the visible absorbance of the wells was measured using a plate reader at 570 nm, while 630 nm was used as a reference wavelength. Cell survival (%) was calculated using the equation of $(A_{570} - A_{630})$ / (control mean) × 100%. Control mean is the average of 10 control wells (medium only). The data were fitted to the normalized dose-response curve (response = 100 / [1 + 10^(($\log_{10}(IC_{50})$ – $\log_{10}$(dose)) × hill slope)])) using GraphPad Prism 6.[37]

2. RESULTS AND DISCUSSION

2.1. Design, Synthesis, and Structure of Carbazoleplatin. We looked into the possibility of using carbazole as part of our new platinum-intercalator conjugate for two reasons: novelty and toxicity. Carbazole is a polyaromatic heterocycle containing two benzene rings fused on either side of a five-membered ring with a nitrogen atom. Carbazole has diverse biological activities, including

antitumor activities.[38] It has been speculated that carbazole may intercalate into DNA helix,[38,39] but carbazole itself has not been used as a DNA intercalating agent in our best knowledge.[40,41] In addition, carbazole is less toxic (LD_{50} >5000 mg/kg) than most of the classical intercalators such as ethidium or acridine.[42] Toxicity is the major limitation of current platinum-intercalator conjugates,[43] so we thought there might be a potential benefit of making a less toxic molecule.

We synthesized [$PtCl(NH_3)_2$(2-(9H-carbazol-9-yl)ethan-1-amine)](NO_3), or carbazoleplatin, from *9H*-carbazole in 5 steps with some modifications of the reported synthetic procedures of monofunctional platinum compounds (Scheme 1A).[44,45] The chemical structure of carbazoleplatin was unambiguously characterized by single crystal X-ray crystallography (Scheme 1B, Table 1). This simple design and efficient synthesis route provide the possibility for facile structural optimizations around the carbazole ring, the linker, and the platinum.

2.2. Crystal Structure of Carbazoleplatin-DNA Adduct. To define the DNA-binding mode of carbazoleplatin, we determined a crystal structure of carbazoleplatin-DNA adduct using human DNA polymerase β host-guest complex (pol *β*-HGC) system, which we had previously used to determine the structure of N7-methylguanine-containing DNA .[26,46] The system enables the facile determination of a three-dimensional structure of a lesion-containing DNA in B-DNA conformation in the absence of a protein contact (Figure 2A).[26,46] A single nucleotide gapped DNA containing N7-carbazoleplatin-G-adduct at the upstream primer was incubated with pol *β* to give a binary complex crystal (Figure 2A). The N7-carbazoleplatin-G binary complex structure, refined at 2.5 Å resolution (Table 2), revealed that the carbazole-platinum conjugate platinated N7 of a guanine, and the carbazole moiety intercalated into two base pairs (Figure 2, PDB ID 5HHI). The long axis of the carbazole moiety was parallel to the long axis of Watson-Crick base pair, thereby making extensive π-π stacking interactions (Figure 2B). The carbazole moiety of carbazoleplatin was predominantly intercalated into two G:C base pairs, as indicated by the strong electron density (Figure 2C). Since platination in general occurs at the N7 of a guanine, the intercalation of carbazole was predicted to occur between G:C and G:C base pairs or between G:C and A:T base pairs. In our pol *β*-HGC experiment setting (5'-TGC-3', G denotes the platination site), the platinated-G:C base pair was

flanked by A:T and G:C. The intercalation of carbazoleplatin was observed at the interface between two G:C base pairs rather than between G:C and A:T base pairs. Is it the base pair or the directionality that primarily influences this intercalation pattern? In the published Pt-ACRAMTU-DNA structure that contains 5'-CGT-3' sequence (G denotes the platination site), its acridine moiety intercalated into 5'-CG-3' rather 5'-GT-3' base pairs.[23] Thus, carbazoleplatin's preferential intercalation into 5'-GC-3' and 5'-CG-3' is likely driven by the surrounding base pairs rather than the directionality. It could be possible that an intercalation into two G:C base pairs is more thermodynamically favorable than an intercalation into G:C and A:T base pairs.

We compared the crystal structure of the carbazoleplatin-containing DNA in pol β to the crystal structure of a lesion-free DNA in pol β (Table 2, PDB ID 5HHH), and it appeared that carbazoleplatin did not induce significant changes in the most of the distortion parameters (Table 3).

2.3. NER Repair Assay of Carbazoleplatin-DNA Adduct. In order to assess the carbazoleplatin-induced helical distortion in a biological context, we tested how efficiently UvrABC endonuclease, the prokaryotic NER system, performs the double incision on carbazoleplatin-containing DNA (Figure 3). We observed that the UvrABC incision rate was approximately 20% per hour when the substrate contained the carbazoleplatin lesion (16% dual incision + 4% single incision, land 6 of Figure 3). In the case of cisplatin 1,2-intrastrand lesion, the incision rate was approximately 45% per hour (34% dual incision + 11% single incision, lane 3 of Figure 3).

Both prokaryotic and eukaryotic NER machineries recognize and/or remove the similar range of lesions through coordinated actions.[47-52] The UvrABC, which is present only in prokaryotes and archaea, has been used as a model system for studying NER efficiency of bulky and/or helix-distorting lesions ranging from pyrimidine dimer to cisplatin intrastrand crosslink adducts.[53] Although prokaryotic NER requires a much less proteins than eukaryotic NER, the both systems employ a very similar strategy including damage recognition, dual incision, repair and ligation. Similar to eukaryotic NER, the UvrABC-mediated repair is a multistep process: (1) damage recognition by $UvrA_2B$ complex, (2) formation of the preincision complex, and (3) UvrC binding and

double incision.[54] A thorough comparison study of the UvrABC's repair efficiency against cisplatin 1,2-intrastrand crosslink to that of 1,3-intrastrand crosslink revealed that the last incision step by UvrABC is the rate-limiting step, but it was found that the nature of the substrate also affect the steps before the incision.[54] In our UvrABC assay, the formation of the single incision and the double incision products of the lane 6 (Figure 3) suggest that carbazoleplatin damage is recognized by $UvrA_2B$ and the preincision complex could be formed on the lesion, but UvrC could not incise the lesion as efficient as the cisplatin 1,2-intrastrand lesion. We speculate the carbarzoleplatin's diminutive distortion of DNA made UvrC difficult to incise the lesion.

2.4. Cell Viability Assay of Carbazoleplatin. We examined antiproliferative activity of carbazoleplatin against human cancer cell lines via MTT cell viability assay. Carbazoleplatin was found to be 5 and 9 times more cytotoxic than cisplatin against pancreatic cancer (PANC-1) and triple negative breast cancer (MDA-MB-231) cell lines, respectively (Table 4). The higher cytotoxicity of carbazoleplatin might result from carbazoleplatin's distinctive mode of action, in which the carbazole intercalation is assisted and stabilized by the platination of monofunctional platinum. The platinum moiety may provide additional specificity toward DNA via its cationic charge and prodrug-like platinum-chloride bond.[22,55]

Although the cytotoxicity data should not be taken literally,[56] the greater cytotoxicity of carbazoleplatin compared to that of cisplatin would serve to warrant the future mechanism of action studies of carbazoleplatin. The cellular uptake of carbazoleplatin could be different from that of cisplatin. While cisplatin's main uptake pathway is passive diffusion,[8] carbazoleplatin bearing the bulky liphophilic carbazole moiety would not be readily transported into the nucleus by passive diffusion, which could influence the cytotoxicity and drug resistance of carbazoleplatin. While cisplatin-DNA adduct formation does not involve intercalation, the N7-carbazoleplatin-dG adduct formation could be facilitated by intercalation, which can interfere with topoisomerase-mediated strand scission and religation. The monofunctional intercalating platinum agent Pt-ACRAMTU has been shown to stall DNA replication, inhibit transcription and induce S-phase arrest.[57] The mechanism of action of carbazoleplatin, a monofunctional-intercalative platinum agent, could be

similar to that of Pt-ACRAMTU. Assessing the effect of carbazoleplatin-DNA adduct on biological processes such as DNA replication, transcription, repair, and topoisomerization in NER-proficient and NER-deficient cells would be required for elucidation of the mechanism of action of carbazoleplatin.

3. CONCLUSIONS

We have reported the synthesis, the structure, and the bioactivity of a platinum-intercalator conjugate (carbazoleplatin). We visualized its DNA binding mode via X-ray, and we also tested how its DNA adduct is repaired by a NER complex. Carbazoleplatin modified the N7 of a guanine, and its carbazole moiety intercalated into the nearby 5'-GC-3' base pairs. Carbazoleplatin induced minimal helical distortion upon DNA modification, and its DNA adduct was less efficiently removed by the UvrABC system than the cisplatin counterpart. These early stage assays enhance our confidence in carrying out more rigorous biochemical and cellular studies of carbazoleplatin in the future.

ACKNOWLEDGMENTS

The research was supported by grant from the Cancer Prevention Research Institute of Texas (Grant RP130219) We are grateful to Dr. Arthur Monzingo for technical assistance. Instrumentation and technical assistance for this work were provided by the Macromolecular Crystallography Facility, with financial support from the College of Natural Sciences, the Office of the Executive Vice President and Provost, and the Institute for Cellular and Molecular Biology at the University of Texas at Austin. The Berkeley Center for Structural Biology is supported in part by the National Institute of General Medical Sciences of the National Institute of Health. The Advanced Light Source is supported by the Director, Office of Science, Office of Basic Energy Sciences, of the U.S. Department of Energy under Contract No. DE-AC02-05CH11231.

CONFLICT OF INTEREST

The authors declare no conflicts of interest.

REFERENCES

[1] M. Galanski, M.A. Jakupec, B.K. Keppler, *Curr. Med. Chem.* **2005**, *12*, 2075.

[2] K. Wang, J.F. Lu, R.C. Li, *Coord. Chem. Rev.* **1996**, *151*, 53.

[3] E.R. Jamieson, S.J. Lippard, *Chem. Rev.* **1999**, *99*, 2467.

[4] P.M. Takahara, A.C. Rosenzweig, C.A. Frederick, S.J. Lippard, *Nature* **1995**, *377*, 649.

[5] P.M. Takahara, C.A. Frederick, S.J. Lippard, *J. Am. Chem. Soc.* **1996**, *118*, 12309.

[6] R.C. Todd, S.J. Lippard, *J. Inorg. Biochem.* **2010**, *104*, 902.

[7] D. Wang, S.J. Lippard, *Nat. Rev. Drug Discov.* **2005**, *4*, 307.

[8] Y. Jung, S.J. Lippard, *Chem. Rev.* **2007**, *107*, 1387.

[9] R.F. Ozols, *Cancer Treat Rev* **1991**, *18 Suppl A*, 77.

[10] Z.H. Siddik, *Oncogene* **2003**, *22*, 7265.

[11] B. Koberle, J.R. Masters, J.A. Hartley, R.D. Wood, *Curr. Biol.* **1999**, *9*, 273.

[12] C. Welsh, R. Day, C. McGurk, J.R. Masters, R.D. Wood, B. Koberle, *Int. J. Cancer* **2004**, *110*, 352.

[13] K.V. Ferry, T.C. Hamilton, S.W. Johnson, *Biochem. Pharmacol.* **2000**, *60*, 1305.

[14] M.J. Cleare, J.D. Hoeschele, *Bioinorganic Chemistry* **1973**, *2*, 187.

[15] T.C. Johnstone, G.Y. Park, S.J. Lippard, *Anticancer Res.* **2014**, *34*, 471.

[16] T.C. Johnstone, K. Suntharalingam, S.J. Lippard, *Chem. Rev.* **2016**, *116*, 3436.

[17] M.V. Keck, S.J. Lippard, *J. Am. Chem. Soc.* **1992**, *114*, 3386.

[18] F. Zunino, G. Savi, A. Pasini, *Cancer Chemother Pharmacol* **1986**, *18*, 180.

[19] E.T. Martins, H. Baruah, J. Kramarczyk, G. Saluta, C.S. Day, G.L. Kucera, U. Bierbach, *J. Med. Chem.* **2001**, *44*, 4492.

[20] M.C. Ackley, C.G. Barry, A.M. Mounce, M.C. Farmer, B.E. Springer, C.S. Day, M.W. Wright, S.J. Berners-Price, S.M. Hess, U. Bierbach, *J. Biol. Inorg. Chem.* **2004**, *9*, 453.

[21] S.M. Hess, A.M. Mounce, R.C. Sequeira, T.M. Augustus, M.C. Ackley, U. Bierbach, *Cancer Chemotherapy and Pharmacology* **2005**, *56*, 337.

[22] H. Baruah, C.G. Barry, U. Bierbach, *Curr. Top. Med. Chem.* **2004**, *4*, 1537.

[23] H. Baruah, M.W. Wright, U. Bierbach, *Biochemistry* **2005**, *44*, 6059.

[24] S. Dutta, M.J. Snyder, D. Rosile, K.L. Binz, E.H. Roll, J. Suryadi, U. Bierbach, M. Guthold, *Cell Biochem Biophys* **2013**, *67*, 1103.

[25] E.Y. Chua, G.E. Davey, C.F. Chin, P. Droge, W.H. Ang, C.A. Davey, *Nucleic Acids Res.* **2015**, *43*, 5284.

[26] Y. Kou, M.C. Koag, S. Lee, *J. Am. Chem. Soc.* **2015**, *137*, 14067.

[27] M.R. Sawaya, R. Prasad, S.H. Wilson, J. Kraut, H. Pelletier, *Biochemistry* **1997**, *36*, 11205.

[28] M.C. Koag, S. Lee, *J. Am. Chem. Soc.* **2014**, *136*, 5709.

[29] A. Tremeau-Bravard, T. Riedl, J.M. Egly, M.E. Dahmus, *J. Biol. Chem.* **2004**, *279*, 7751.

[30] V.K. Batra, W.A. Beard, D.D. Shock, J.M. Krahn, L.C. Pedersen, S.H. Wilson, *Structure* **2006**, *14*, 757.

[31] Z. Otwinowski, W. Minor, *Methods Enzymol.* **1997**, *276*, 307.

[32] P. Emsley, K. Cowtan, *Acta Crystallogr D Biol Crystallogr* **2004**, *60*, 2126.

[33] P.D. Adams, R.W. Grosse-Kunstleve, L.W. Hung, T.R. Ioerger, A.J. McCoy, N.W. Moriarty, R.J. Read, J.C. Sacchettini, N.K. Sauter, T.C. Terwilliger, *Acta Crystallogr D Biol Crystallogr* **2002**, *58*, 1948.

[34] X.J. Lu, W.K. Olson, *Nucleic Acids Res.* **2003**, *31*, 5108.

[35] D. Pakotiprapha, Y. Inuzuka, B.R. Bowman, G.F. Moolenaar, N. Goosen, D. Jeruzalmi, G.L. Verdinel, *Mol. Cell* **2008**, *29*, 122.

[36] W. Rasband. (1997) ImageJ. US National Institutes of Health, Bethesda, Maryland. *ImageJ. US National Institutes of Health, Bethesda, Maryland*. Available.

[37] One-way ANOVA followed by Dunnett's multiple comparisons test was performed using GraphPad Prism version 6.00 for Windows. *One-way ANOVA followed by Dunnett's multiple comparisons test was performed using GraphPad Prism version 6.00 for Windows*. GraphPad Software, La Jolla, California, USA.

[38] M.S. Shaikh, R. Karpoormath, N. Thapliyal, R.A. Rane, M.B. Palkar, A.M. Faya, H.M. Patel, W.S. Alwan, K. Jain, G.A. Hampannavar, *Anti-Cancer Agents in Medicinal Chemistry* **2015**, *15*, 1049.

[39] R. Rajagopalan, T.S. Lin, A.S. Karwa, A.R. Poreddy, B. Asmelash, R.B. Dorshow, *ACS Med Chem Lett* **2012**, *3*, 284.

[40] H.J. Knolker, K.R. Reddy, *Chem. Rev.* **2002**, *102*, 4303.

[41] B.L. Staker, M.D. Feese, M. Cushman, Y. Pommier, D. Zembower, L. Stewart, A.B. Burgin, *J. Med. Chem.* **2005**, *48*, 2336.

[42] E. Eagle, A.J. Carlson, *J. Pharmacol. Exp. Ther.* **1950**, *99*, 450.

[43] J. Suryadi, U. Bierbach, *Chem. Eur. J.* **2012**, *18*, 12926.

[44] L.S. Hollis, A.R. Amundsen, E.W. Stern, *J. Med. Chem.* **1989**, *32*, 128.

[45] G.Y. Park, J.J. Wilson, Y. Song, S.J. Lippard, *Proc Natl Acad Sci U S A* **2012**, *109*, 11987.

[46] B.R. Bowman, S. Lee, S. Wang, G.L. Verdine, *Structure* **2008**, *16*, 1166.

[47] L. Galluzzi, L. Senovilla, I. Vitale, J. Michels, I. Martins, O. Kepp, M. Castedo, G. Kroemer, *Oncogene* **2012**, *31*, 1869.

[48] S.G. Chaney, A. Sancar, *J. Natl. Cancer Inst.* **1996**, *88*, 1346.

[49] T. Furuta, T. Ueda, G. Aune, A. Sarasin, K.H. Kraemer, Y. Pommier, *Cancer Res.* **2002**, *62*, 4899.

[50] A.F. Fagbemi, B. Orelli, O.D. Scharer, *DNA Repair (Amst)* **2011**, *10*, 722.

[51] J.A. Marteijn, H. Lans, W. Vermeulen, J.H. Hoeijmakers, *Nat. Rev. Mol. Cell Biol.* **2014**, *15*, 465.

[52] C. Kisker, J. Kuper, B. Van Houten, *Cold Spring Harb Perspect Biol* **2013**, *5*, a012591.

[53] S.F. Bellon, J.H. Coleman, S.J. Lippard, *Biochemistry* **1991**, *30*, 8026.

[54] R. Visse, A.J. van Gool, G.F. Moolenaar, M. de Ruijter, P. van de Putte, *Biochemistry* **1994**, *33*, 1804.

[55] T.C. Johnstone, J.J. Wilson, S.J. Lippard, *Inorg. Chem.* **2013**, *52*, 12234.

[56] J. van Meerloo, G.J. Kaspers, J. Cloos, *Methods Mol Biol* **2011**, *731*, 237.

[57] J. Suryadi, U. Bierbach, *Chem. Eur. J.* **2012**, *18*, 12926

FIGURES

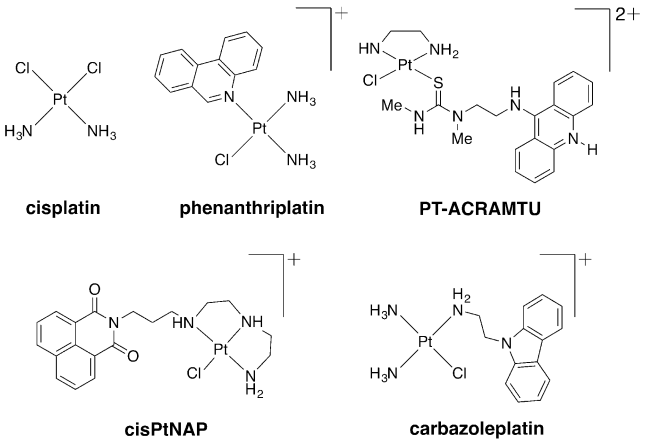

Figure 1. Cisplatin and monofunctional platinum-based anticancer agents.

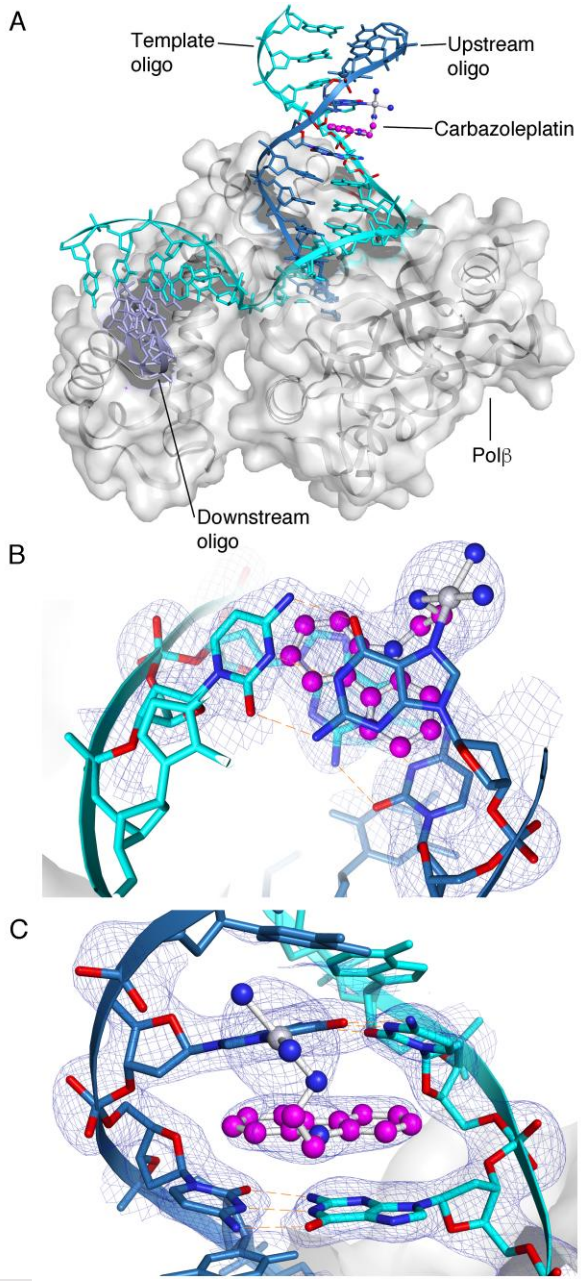

Figure 2. Structure of carbazoleplatin-G adduct determined by human DNA polymerase *β* host-guest complex (pol *β*-HGC) system. (A) The X-ray structure of pol *β*-HGC with carbazoleplatin-DNA adduct showing both the platination and the intercalation of carbazoleplatin (white: pol *β*, teal: template, blue: upstream primer, violet: downstream primer, magenta: carbazoleplatin) (B) A top view showing the platination of guanine N7 by carbazoleplatin. The electron density map (2Fo - Fc) was contoured at 1.0 σ around carbazoleplatin and its neighboring DNA bases. (C) A side view showing the intercalation of carbazoleplatin into the platinated G:C and the next G:C base pairs. The electron density map ($2F_o$ - F_c) was contoured at 1.0 σ around carbazoleplatin and its neighboring DNA bases.

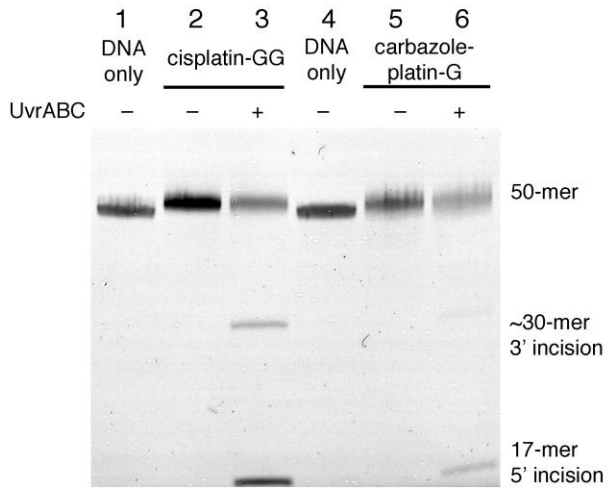

Figure 3. UvrABC dual incision assay of the cisplatin 1,2-intrastrand crosslink adduct and the carbazoleplatin adduct. 50-mer duplex DNA containing either a cisplatin-GG or a carbazoleplatin-G adduct were used. Lane descriptions: (1) Unmodified 50-mer duplex DNA. (2) Cisplatin 1,2-intrastrand crosslink-containing duplex DNA in the absence of UvrABC. (3) Cisplatin 1,2-intrastrand crosslink-containing duplex DNA in the presence of UvrABC. (4) Unmodified duplex DNA. (5) Carbazoleplatin-containing duplex DNA in the absence of UvrABC. (6) Carbazoleplatin-containing DNA in the presence of UvrABC.

SCHEMES

Scheme 1. Synthesis and Single Crystal X-ray Structure of Carbazoleplatin[α]

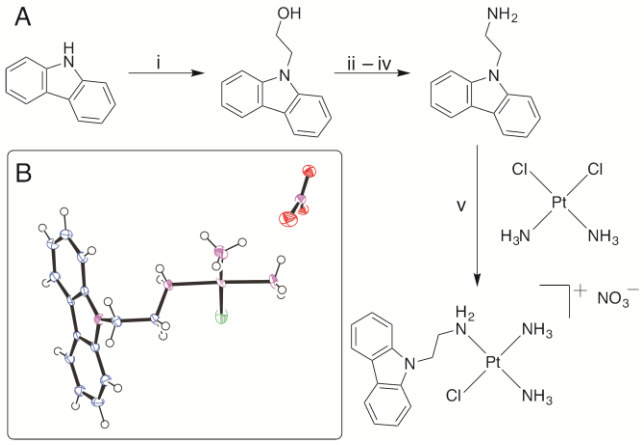

[α](*A*) Preparation of carbazoleplatin (i) KOH, 2-bromoethanol, acetone, reflux, dark, 32%; (ii) I_2, imidazole, PPh_3, THF; (iii) NaN_3, DMF, 70ºC, 58% (over 2 steps); (iv) PPh_3, H_2O, THF, 58%; (v) the reaction product of *cis*-Diamminedichloridoplatinum(II) and $AgNO_3$, DMF, 55ºC, dark, 23%. (*B*) Single crystal X-ray structure of carbazoleplatin and its nitrate counter ion.

TABLES

Table 1. Crystallographic Data for Carbazoleplatin

chemical formula	C14 H20 Cl N5 O3 Pt
formula weight	536.88
temperature	100(2) K
wavelength	1.54184 Å
crystal system	monoclinic
space group	P21/n
unit cell dimensions	
a = 17.6087(3) Å	α = 90°
b = 5.45090(10) Å	β = 96.5600(10)°
c = 36.3822(5) Å	γ = 90°
volume	3469.22(10) $Å^3$
Z	8
density (calculated)	2.071 Mg/m^3
absorption coefficient	16.780 mm^{-1}
F(000)	2080
crystal size	0.180 × 0.110 x 0.040 mm^3
theta range for data collection	2.445 to 74.271°.
index ranges	–21 ≤ h ≤ 21 –6 ≤ k ≤4 –45 ≤ l ≤ 45
reflections collected	18275
independent reflections	6857 [R(int) = 0.0242]

completeness to theta = 67.684°	99.5 %
absorption correction	Semi-empirical from equivalents
max. and min. transmission	1.00 and 0.585
refinement method	Full-matrix least-squares on F^2
data / restraints / parameters	6857 / 566 / 476
goodness-of-fit on F^2	1.099
final R indices [I>2sigma(I)]	R1 = 0.0328, wR2 = 0.0680
R indices (all data)	R1 = 0.0371, wR2 = 0.0690
extinction coefficient	n/a
largest diff. peak and hole	1.358 and -1.601 e.$Å^{-3}$

Table 2. Data Collection and Refinement Statistics for pol *β*-carbazoleplatin Host-Guest Complex

	5HHH	5HHI
PDB code	G:C	Carbazoleplatin -G:C
Data Collection		
Space Group	$P2_1$	$P2_1$
Cell constants		
a (Å)	51.334	54.372
b	84.595	80.119
c	55.523	54.674
α (º)	90.00	90.00
β	107.494	108.942
γ	90.00	90.00
Resolution (Å)[a]	20-2.36	20-2.52
	(2.41-2.36)	(2.56-2.52)
R_{merge}[b] (%)	0.080	0.075
	(0.359)	(0.380)
<I/σ>	20.7 (2.73)	22.0 (2.50)
Completeness (%)	100 (99.9)	99.3 (93.4)
Redundancy	3.7 (3.7)	4.8 (4.3)
Refinement		
R_{work}[c]/R_{free}[d] (%)	21.2/26.2	22.4/27.8
Unique reflections	18516	14873
Mean B factor ($Å^2$)		
Protein	44.7	53.5

Ligand	37.5	64.3
Solvent	40.8	43.1
Ramachandran plot		
Most favored (%)	96.6	94.1
Additional allowed (%)	3.4	5.6
RMSD		
Bond lengths (Å)	0.005	0.005
Bond angles (º)	0.710	0.680

[a] Values in parentheses are for the highest resolution shell.

[b] $R_{merge} = \Sigma|I-\langle I\rangle|/\Sigma I$ where I is the integrated intensity of a given reflection.

[c] $R_{work} = \Sigma|F(obs)-F(calc)|/ \Sigma F(obs)$.

[d] $R_{free} = \Sigma|F(obs)-F(calc)|/ \Sigma F(obs)$, calculated using 5% of the data.

Table 3. DNA Torsion Analysis of the Carbazoleplatin-G Structure

Distortion parameter	Control DNA (5HHH) (º)	Carbazoleplatin-DNA (5HHI) (º)	Difference (º)
Shear	–0.41	–0.05	0.36
Stretch	–0.01	–0.15	0.14
Stagger	0.24	0.09	0.15
Buckle	–4.05	0.61	4.66
Propeller	–7.1	–7.05	0.05
Opening	–1.19	–2.15	0.96
Shift	0.35	–0.28	0.63
Slide	–0.35	0.28	0.63
Rise	3.19	3.03	0.16
Tilt	1.52	–3.01	4.53
Roll	4.27	4.19	0.08
Twist	34.13	32.33	1.80
x-Displacement	–1.3	–0.28	1.02
y-Displacement	–0.34	–0.03	0.31
Helical rise	3.18	2.96	0.22
Inclination	7.27	7.57	0.30
Tip	–2.57	5.51	8.08
Twist	34.79	33.08	1.71

Table 4. Cytotoxicity Profile of Carbazoleplatin and Cisplatin

Cell line (Cancer type)	IC_{50} (μM)[a]	
	Carbazoleplatin	Cisplatin
PANC-1 (Pnacreas)	5.3	43.3
MDA-MB-231 (Breast)	9.3	47.5

[a]Each IC_{50} was calculated by averaging 4 replicates.

SUPPORTING INFORMATION

Spectral data, X-ray crystallography tables, and MTT cytotoxicity graphs are included the supporting information.

GRAPHICAL TABLE OF CONTENTS

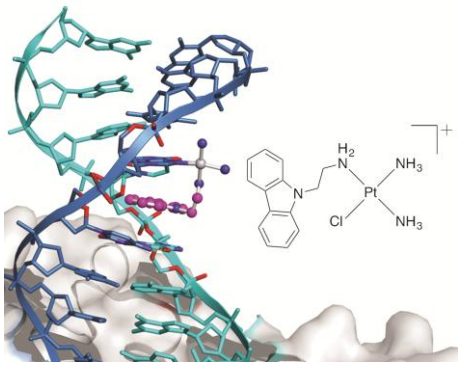

We designed and synthesized a monofunctional platinum-carbazole conjugate (carbazoleplatin). The crystal structure of carbazoleplatin-DNA adduct showed that carbazoleplatin modified N7 of a guanine (G) base and intercalated into two G:C base pairs without significantly distorting the double helix. UvrABC removed the carbazoleplatin-containing DNA less efficiently than the cisplatin 1,2-intrastrand crosslink-containing DNA. Carbazoleplatin was several-fold more cytotoxic than cisplatin in PANC-1 and MDA-MB-231 cell lines.